

Spectroscopic study of $B^2\Sigma^+$--$X_1^2\Pi_{1/2}$ transition of electron electric dipole moment candidate PbF

Ben Chen(陈犇), Yi-Ni Chen(陈旖旎), Jia-Nuan Pan(潘佳煖), Jian-Ping Yin(印建平), and Hai-Ling Wang(汪海玲)
Citation: Chin. Phys. B, 2022, 31 (**9**): 093301. DOI: 10.1088/1674-1056/ac633a
Journal homepage: http://cpb.iphy.ac.cn; http://iopscience.iop.org/cpb

What follows is a list of articles you may be interested in

Laser-induced fluorescence experimental spectroscopy and theoretical calculations of uranium monoxide

Xi-Lin Bai(白西林), Xue-Dong Zhang(张雪东), Fu-Qiang Zhang(张富强), and Timothy C Steimle
Chin. Phys. B, 2022, 31 (**5**): 053301. DOI: 10.1088/1674-1056/ac43a4

Hyperfine structures and the field effects of IBr molecule in its rovibronic ground state

Defu Wang(王得富), Xuping Shao(邵旭萍), Yunxia Huang(黄云霞), Chuanliang Li(李传亮), and Xiaohua Yang(杨晓华)
Chin. Phys. B, 2021, 30 (**11**): 113301. DOI: 10.1088/1674-1056/abfc3d

Stark effect of the hyperfine structure of ICl in its rovibronic ground state: Towards further molecular cooling

Qing-Hui Wang(王庆辉), Xu-Ping Shao(邵旭萍), Xiao-Hua Yang(杨晓华)
Chin. Phys. B, 2016, 25 (**1**): 013301. DOI: 10.1088/1674-1056/25/1/013301

High-resolution photoassociation spectroscopy of ultracold Cs_2 long-range 0_g^- state： The external well potential depth

Liu Wen-Liang, Wu Ji-Zhou, Ma Jie, Xiao Lian-Tuan, Jia Suo-Tang
Chin. Phys. B, 2014, 23 (**1**): 013301. DOI: 10.1088/1674-1056/23/1/013301

High resolution photoassociation spectra of an ultracold Cs_2 long-range 0_u^+ ($6S_{1/2}$+$6P_{1/2}$) state

Chen Peng, Li Yu-Qing, Zhang Yi-Chi, Wu Ji-Zhou, Ma Jie, Xiao Lian-Tuan, Jia Suo-Tang
Chin. Phys. B, 2013, 22 (**9**): 093301. DOI: 10.1088/1674-1056/22/9/093301

Spectroscopic study of $B^2\Sigma^+$–$X_1{}^2\Pi_{1/2}$ transition of electron electric dipole moment candidate PbF

Ben Chen(陈犇), Yi-Ni Chen(陈旖旎), Jia-Nuan Pan(潘佳煖),
Jian-Ping Yin(印建平), and Hai-Ling Wang(汪海玲)†

State Key Laboratory of Precision Spectroscopy, East China Normal University, Shanghai 200241, *China*

(Received 2 February 2022; revised manuscript received 20 March 2022; accepted manuscript online 1 April 2022)

PbF, a valuable candidate for measuring the electron electric dipole moment (eEDM), is of great significance in measuring its spectrum and deriving its molecular constants in experiment. In the present work, the rovibronic spectrum of the $B^2\Sigma^+$–$X_1{}^2\Pi_{1/2}$ transition of PbF in a wavelength range of 260 nm–285 nm is studied by the laser ablation/laser induced fluorescence method. The molecular parameters of the $X_1{}^2\Pi_{1/2}$ ($v''=0$) and $B^2\Sigma^+$ ($v'=0,1$) states are derived from the recorded spectra of the (0, 0) and (1, 0) bands of the $B^2\Sigma^+$–$X_1{}^2\Pi_{1/2}$ transition. Also, the Franck–Condon factors (FCFs) of the transitions between the $B^2\Sigma^+$ and $X_1{}^2\Pi_{1/2}$ states are calculated by the RKR/LEVEL method and the Morse potential method, respectively.

Keywords: spectroscopic parameters, Franck–Condon factors, an eEDM candidate, lifetime

PACS: 33.15.Pw, 33.20.Lg, 33.20.Vq, 33.70.Ca **DOI:** 10.1088/1674-1056/ac633a

1. Introduction

Heavy polar diatomic molecule, PbF, with a single unpaired electron and a larger internal electric field ($E_{\rm eff}$), is a valuable and sensitive candidate for measuring the electron electric dipole moment (eEDM) accurately.[1–3] Spectroscopic experimental study of open shell state of PbF is required for implementing the precise eEDM measurement.

The preliminary study of the B–X_1 emission spectrum of PbF was first conducted by Rochester in a carbon tube furnace in 1938.[4] Reddy and Rao have photographed the B–X_2 subsystem in the 2$^{\rm nd}$ order of a 21-ft (1 ft = 3.048×10^{-1} cm^{-1}) concave grating spectrogram, but in their spectra the fine structure is not well-resolved.[5] Later, Singh and Singh determined the rotational constants of the upper and lower states, B and X_2 states.[6] In 1977, Lumley and Barrow studied the rotational transitions of the B–X_1 system of PbF in a King furnace by the spectrograph method and gave the rotational constants for the B and X_1 states.[7] In 1985, Balasubramanian used the relativistic configuration interaction approach to calculate the low-lying states of PbF and gave the associated potential curves.[8] In 1992, Chen and Dagdigian produced PbF by reacting Pb atoms with F_2 molecules, detected the B–X spectrum of PbF by laser-induced fluorescence method, and made a rough estimate of the lifetime of the B state.[9] Ziebarth *et al.* studied the high-resolution emission spectra of PbF in $X_2{}^2\Pi_{3/2}$–$X_1{}^2\Pi_{1/2}$ transition.[10] In addition, the radiative lifetime of the B state of PbF and the average transition dipole moment of B–X_1 transition were given by McRaven *et al.*[11] In 2010, McRaven *et al.* used resonance enhanced multi-photon ionization (REMPI) technique to measure the rotational spectra of the B, D, E, and F states of ^{208}PbF, and determined spectroscopic constants for these states and for the isotopologues ^{206}PbF and ^{207}PbF[12] as well. In a recent study, Baturo *et al.* reported the electric-field-dependent g factor of ^{207,208}PbF's lowest rotational energy level through experimental measurements and theoretical calculations, and gave the optimal electric field of eEDM measurement.[13] However, the reported spectral data of B–X_1 transition of PbF are still meager. Only partial parameters of PbF in B state were given by above studies, the rovibronic spectra and structures of the PbF B–X_1 transition still need studying further.

In this work, the spectra of (0, 0) and (1, 0) bands of PbF in B–X_1 transition are recorded and analyzed to obtain the rovibronic structure and spectral constants of the B state and X_1 state. Also, the FCFs of the transitions between the vibrational levels of the B–X_1 transition and the potential energy curves of B and X_1 states are calculated by the Morse potential method[14] and RKR/LEVEL[15–20] methods.

2. Experiment setup

In the present work, the laser ablation and laser induced fluorescence techniques were used for generating PbF radical and measuring the spectrum of PbF in the range of 260 nm–285 nm. The details of the experimental setup are described in the following.

The PbF molecular beam was produced by the reaction of Pb plasma with CF_4 gas. The ablation laser with a wavelength of 1064 nm and the laser output energy of $\sim$ 1 mJ was focused on $\sim$ 0.5 cm above the rotating and translating Pb metal rod through a lens with a focal length of 30 cm to generate Pb

†Corresponding author. E-mail: hlwang@phy.ecnu.edu.cn

© 2022 Chinese Physical Society and IOP Publishing Ltd

plasma. The reaction gases (10% CF_4 gas mixing with argon carrier gas in volume) were ejected into the reaction chamber from the pulse valve and reacted with the Pb plasma at a distance of 1 cm from the pulse valve to generate PbF molecular beam.

The fluorescence spectrum of $B^2\Sigma^+$–$X_1{}^2\Pi_{1/2}$ transition of the PbF molecules was excited by an excitation laser at a distance of 30 cm from the ablation point. The excitation laser was an Nd:YAG laser pumped dye laser with a typical linewidth of 0.04 cm^{-1} for the fundamental beam. The diameter of the excitation laser beam in the detection chamber was $\sim$ 1 mm. Typical laser pulse energy for detecting the $B^2\Sigma^+$–$X_1{}^2\Pi_{1/2}$ transition of PbF was $\sim$ 0.5 mJ. Typically, the static pressure and the dynamic pressure of the reaction chamber were 3.5×10^{-6} Pa and 5.0×10^{-3} Pa, respectively. The static pressure and the dynamic pressure of the detection chamber were 2.0×10^{-6} Pa and 2.0×10^{-4} Pa, respectively.

The laser excited fluorescence signal was collected with a lens telescope system onto a photomultiplier. The signal from the photomultiplier was directed to a gated integrator. A 1-GHz digital oscilloscope was used to measure the radiative lifetime of the $v'=0$ level and the $v'=1$ level of PbF $B^2\Sigma^+$ state.

The wavenumbers of the spectral lines were calibrated by a calibrated wavemeter.

3. Results and discussion

The B–X_1 transition of PbF is expected to be the $^2\Sigma^+$–$^2\Pi_{1/2}$ transition, each band has six branches. Figure 1 shows the schematic diagram of energy level transitions between the $^2\Sigma^+$ state and $^2\Pi_{1/2}$ state. These six branches are denoted as Q_{21}, Q_1, P_{21}, R_1, P_1, and R_{21}.

As shown in Fig. 1, the allowed transitions are those with $\Delta J=0,\pm1$. Transitions for which $\Delta J=J'-J''=-1$ belongs to the P-branch, $\Delta J=J'-J''=0$ the Q-branch, and $\Delta J=J'-J''=+1$ the R-branch.

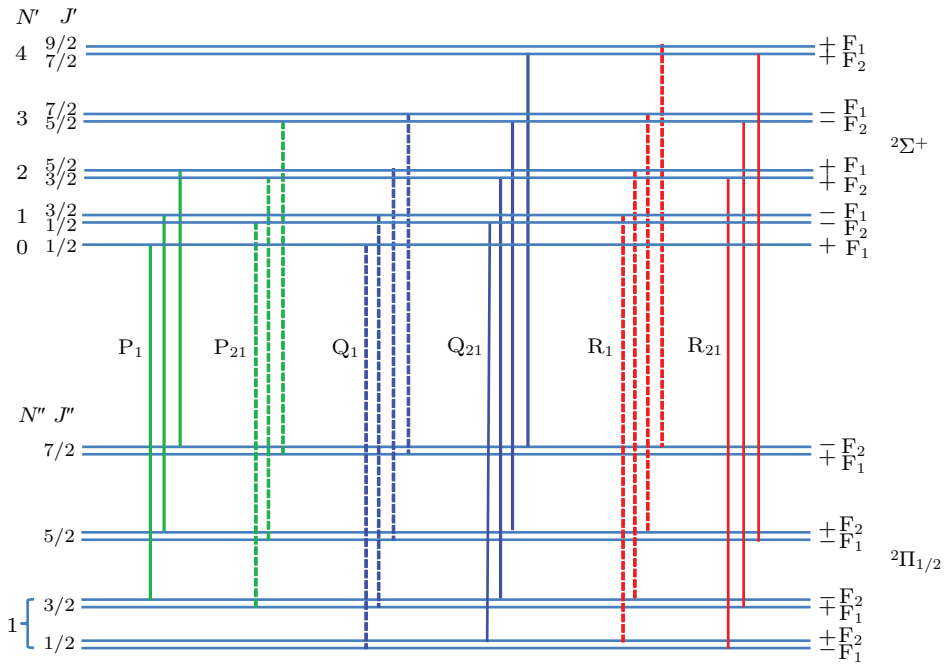


Fig. 1. Schematic diagram of energy levels of B–X_1 transition of ^{208}PbF.

The heavy-metal nature of Pb is reflected clearly in the large spin–orbit splitting in the ground electronic state. The predominant electronic configuration of the X state is found to be $\sigma^2\pi^4\pi^*$. The large spin–orbit splitting in the X state arises from electron occupation in the π^* orbital. The Hamiltonian of the ground state, $X_1{}^2\Pi_{1/2}$, can be expressed as

$$H_{X_1}=B''J''\left(J''+1\right)-D''J''^2\left(J''+1\right)^2\pm\frac{1}{2}p''\left(J''+\frac{1}{2}\right), \quad (1)$$

where B'' and D'' are the rotational constant and the centrifugal distortion, respectively, p'' is the Ω-doubling constant, and J'' is the rotational quantum number.

The B state is assigned as a Rydberg state which stems from the electronic configuration $\sigma^2\pi^4\sigma_R$, with the σ_R orbital being derived from a 7s atomic orbital.[7–9] According to the Barrow's reported results,[21] $B^2\Sigma^+$ is a case (b) state, with very small spin splitting. The Hamiltonian of the B state can be written as[21]

$$H_B(1)=B'J'\left(J'+1\right)-D'J'^2\left(J'+1\right)^2+\frac{1}{2}\gamma J', \quad (2)$$

$$H_B(2)=B'J'\left(J'+1\right)-D'J'^2\left(J'+1\right)^2-\frac{1}{2}\gamma(J'+1), \quad (3)$$

where B' and D' are the rotational constant and the centrifugal distortion, respectively, γ is spin doubling constant, and J' is

the rotational quantum number.

The population of the rotational levels is given by a Boltzmann distribution,

$$P(J,p)=\frac{(2J+1)\exp(-E_{\rm B}(J,p)/k_{\rm B}T)}{\sum_{J_i,p_i}((2J_i+1)\exp(-E_{\rm B}(J_i,p_i)/k_{\rm B}T))}, \quad (4)$$

where p is the parity of the related state, the subscript i refers to the i-th energy level, $k_{\rm B}$ denotes the Boltzmann constant, T represents the rotational temperature of the molecule.

The relative dipole moment between two different states is given by[22]

$$I(v) = \sum_{J''p'',J'p'} P(J'',p'')S \sum_{J''p'',J'p'} \times \exp\left[\frac{-4ln2\left(v_{\rm laser}-v_{J''p'',J'p'}\right)^2}{\Delta v^2}\right], \quad (5)$$

where $v_{J''p'',J'p'}$ is the transition frequency between the upper state $J'p'$ and the lower state $J''p''$, and given in Eq. (6); S is the relative transition dipole moment between the upper state and the lower state, symbol $''$ and symbol $'$ represent the upper state and lower state, respectively.

$$v_{J''p'',J'p'} = \frac{E_{\rm B}(J',p')-E_{X_1}(J'',p'')}{h}. \quad (6)$$

From Eqs. (4) and (5), the calculated relative intensity of Q_{21} branch is around twice stronger than that of the P_1 branch and the R_{21} branch, and the intensity of the P_1 branch and R_{21} branch are almost similar to each other.

The $B^2\Sigma^+$–$X_1{}^2\Pi_{1/2}$ transition of the PbF molecule is a perpendicular transition as deduced by Lumley and Barrow.[7] Figure 2 gives the recorded experimental and simulated spectra of the PbF $B^2\Sigma^+$–$X_1{}^2\Pi_{1/2}$ (1, 0) and (0, 0) bands, respectively.

As shown in Fig. 2, the simulated spectra of (0, 0) and (1, 0) are in good agreement with the experimental ones. The recorded experimental spectra of the (0, 0) and (1, 0) bands of the B–X_1 system are both double-headed. The spectra features have a sharp cut-off in intensity at the lowest transition frequency, and a gradual loss. The spectra are blue-degraded, thus the rotational constants are inequal: $B'(B^2\Sigma^+) > B''(X_1{}^2\Pi_{1/2})$.

The relatively weak spectra on the left-side of (0, 0) and (1, 0) bands belong to the P_1 branches, the ones in the middle are mainly for the Q branch and Q_{21} branch, and the ones on the right side are for the R branch and R_{21} branch. However, under our present experimental conditions only three branches, P_1, Q_{21}, and R_{21}, are resolvable. From the recorded spectra (Fig. 2), the intensity of experimentally measured P_1 branch and R_{21} branch are weaker, the intensity of Q_{21} branch is approximately twice stronger than that of the P_1 branch and the R_{21} branch. These are consistent with our calculated values from Eq. (5).

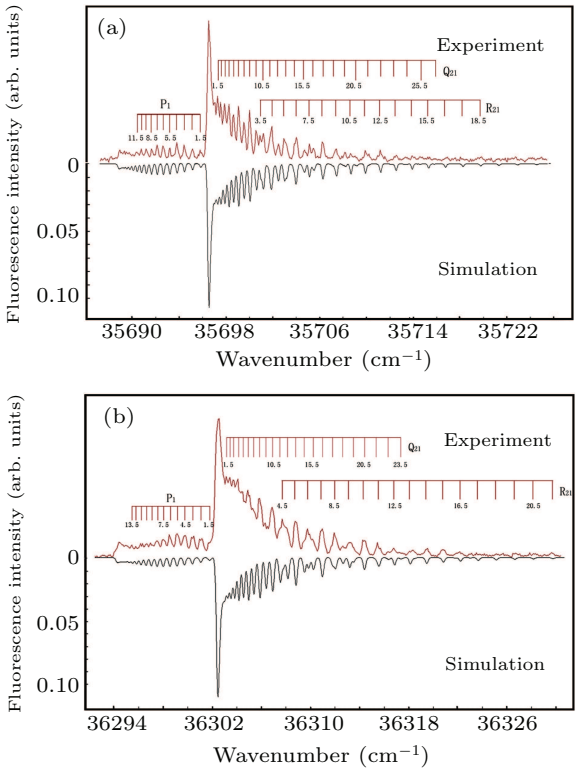


Fig. 2. Experimental (red) and simulated (black) LIF excitation spectra of PbF $B^2\Sigma^+$–$X_1{}^2\Pi_{1/2}$ transition for (a) (0, 0) band and (b) (1, 0) band.

The rovibronic spectra of these two bands, $(0,0)$ and $(1,0)$ (in Fig. 2), are simulated using Pgopher program.[23] The rotational and fine structure constants are determined by directly fitting the experimental data of each band. The derived spectral parameters of the B and X_1 states are given in Table 1.

Table 1. Spectral parameters of $B^2\Sigma^+$ states and $X_1{}^2\Pi_{1/2}$ states of ^{208}PbF (in units of cm^{-1}).

Parameters	$X_1{}^2\Pi_{1/2}$		$B^2\Sigma^+$			
	$v''=0$		$v'=0$		$v'=1$	
	This work	Ref. [10]	This work	Ref. [7]	This work	Ref. [7]
$T_{\rm e}$	0	0	35644.26(8)	35643[a]		
$B_{\rm v}$	0.23066(2)	0.230663(2)	0.24709(12)	0.24736(5)	0.24588(10)	0.24588(5)
$10^7 D_{\rm v}$	1.772(3)	1.823(5)	1.622(9)	1.62(3)	1.455(7)	1.64(3)
p	–0.1382(2)	0.13820(1)				
γ			–0.0098(1)	0.0026(1)	0.0023(4)	0.0027(1)

[a]This value is cited from Table 4 in Ref. [7].

In Herzberger's book, it is mentioned that the B state of PbCl and PbBr is easy to predissociate and assigned as a diffuse band.[24] According to our measurement, the B state of PbF has a short lifetime. It may also be caused by predissociation similar to the case for the B state of PbCl and PbBr. In the present work, we also find that we can excite PbF from its X_1 state to B state by using much lower laser energy than from its X_1 state to A state. It is because the oscillator strengths of the corresponding band systems are relatively great.[9]

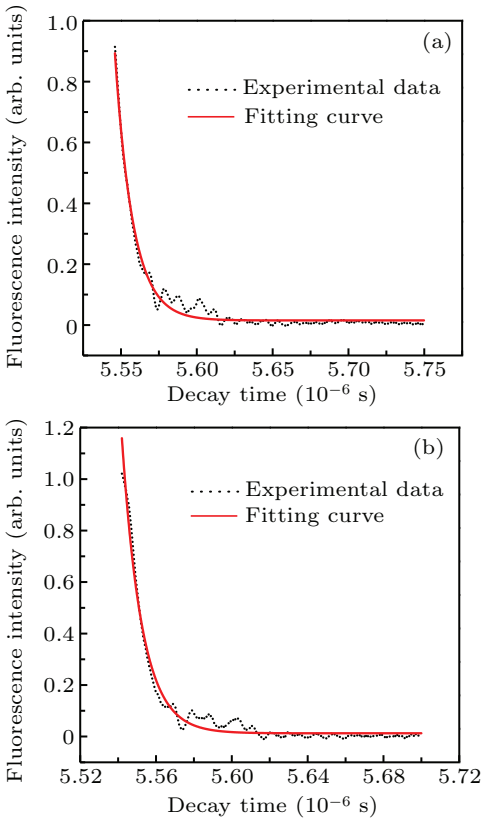


Fig. 3. Decay profile for excitation of (a) $v' = 0$ level and (b) $v' = 1$ level of the B state of PbF, with black dots denoting measured experimental decay data, and red solid lines referring to fitting curves.

Figure 3 displays a typical decay profile for excited B state of PbF molecule. The contributions due to the laser scattered light from the excitation laser and the ablation laser are eliminated in the decay profile which is shown in Fig. 3. The fluctuation of the decay profile results from the fluctuation of the laser output power.

The best fits yielded lifetimes for the B state $v' = 0$ and l levels are 11.90 ns and 10.51 ns, respectively. The duration of the probe laser pulse and the response time of the photomultiplier in the present experiment are both ~ 10 ns. It was shown in Ref. [9] that the lifetime for the $v' = 0$ level and the $v' = 1$ level are 3.6 ± 0.4 ns and 6.6 ± 0.4 ns, respectively. It was estimated in Ref. [11] that the lifetime of the B state is less than 2 ns. To accurately measure the lifetime of the vibrational level of the B state, a laser with a narrow band width or a CW laser, and a rapid response detector are needed.

The potential energy curve of B state is calculated by the Morse potential and RKR/LEVEL methods, and the obtained results are shown in Fig. 4. The calculated FCFs of the B–X_1 transition are shown in Table 2. The calculated FCFs by Morse potential and RKR/LEVEL methods are consistent with each other. The calculated results show that the intensity of the (0, 0) band and the (1, 0) band are similar. The transition intensity of (2, 0) is around half that of the (0, 0) and the (1, 0).

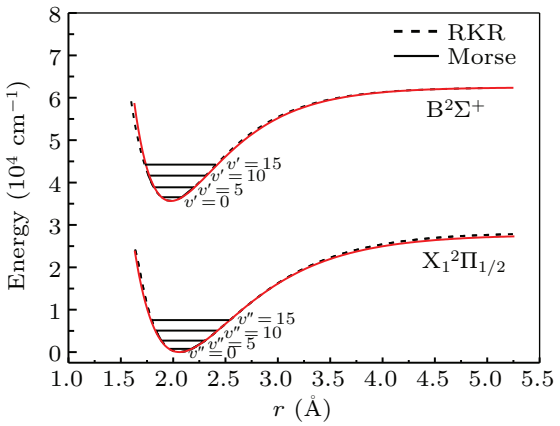


Fig. 4. Calculated potential energy curves of PbF X_1 state and B state by Morse potential (red line) and RKR/LEVEL (black line) methods.

Table 2. Calculated Franck–Condon factors of PbF $B^2\Sigma^+$–$X_1{}^2\Pi_{1/2}$ transition.

	Method	$v' = 0$	$v' = 1$	$v' = 2$	$v' = 3$	$v' = 4$	$v' = 5$	$v' = 6$
$v'' = 0$	Morse	3.86×10^{-1}	3.86×10^{-1}	1.74×10^{-1}	4.55×10^{-2}	7.48×10^{-3}	7.87×10^{-4}	5.16×10^{-5}
	RKR	3.83×10^{-1}	3.84×10^{-1}	1.76×10^{-1}	4.78×10^{-1}	8.29×10^{-3}	9.14×10^{-4}	6.13×10^{-5}
$v'' = 1$	Morse	3.51×10^{-1}	1.17×10^{-3}	2.35×10^{-1}	2.68×10^{-1}	1.15×10^{-1}	2.63×10^{-2}	3.50×10^{-3}
	RKR	3.49×10^{-1}	6.00×10^{-4}	2.27×10^{-1}	2.70×10^{-1}	1.21×10^{-1}	2.86×10^{-2}	3.79×10^{-3}
$v'' = 2$	Morse	1.76×10^{-1}	1.78×10^{-1}	7.25×10^{-2}	6.93×10^{-2}	2.60×10^{-1}	1.80×10^{-1}	5.54×10^{-2}
	RKR	1.76×10^{-1}	1.70×10^{-1}	8.10×10^{-2}	5.98×10^{-2}	2.58×10^{-1}	1.88×10^{-1}	5.76×10^{-2}
$v'' = 3$	Morse	6.34×10^{-2}	2.24×10^{-1}	3.30×10^{-2}	1.49×10^{-1}	2.77×10^{-3}	1.94×10^{-1}	2.23×10^{-1}
	RKR	6.52×10^{-2}	2.21×10^{-1}	2.52×10^{-2}	1.58×10^{-1}	8.97×10^{-4}	1.93×10^{-1}	2.31×10^{-1}
$v'' = 4$	Morse	1.83×10^{-2}	1.34×10^{-1}	1.67×10^{-1}	8.75×10^{-4}	1.50×10^{-1}	1.35×10^{-2}	1.16×10^{-1}
	RKR	1.98×10^{-2}	1.37×10^{-1}	1.55×10^{-1}	3.67×10^{-3}	1.53×10^{-1}	1.73×10^{-2}	1.24×10^{-1}
$v'' = 5$	Morse	4.45×10^{-3}	5.46×10^{-2}	1.68×10^{-1}	8.35×10^{-2}	3.38×10^{-2}	1.04×10^{-1}	5.53×10^{-2}
	RKR	5.21×10^{-3}	5.92×10^{-2}	1.67×10^{-1}	6.81×10^{-2}	4.48×10^{-2}	1.05×10^{-1}	5.62×10^{-2}
$v'' = 6$	Morse	9.29×10^{-4}	1.73×10^{-2}	9.54×10^{-2}	1.59×10^{-1}	2.31×10^{-2}	7.72×10^{-2}	5.01×10^{-2}
	RKR	1.24×10^{-3}	2.04×10^{-2}	1.01×10^{-1}	1.49×10^{-1}	1.44×10^{-2}	8.76×10^{-2}	5.89×10^{-2}

4. Conclusions

In this work, the laser ablation technique combining with the chemical reaction method is used to produce PbF radicals. The rovibronic spectra of (0, 0) and (1, 0) bands of PbF $B^2\Sigma^+$–$X_1{}^2\Pi_{1/2}$ transition in a range of 260 nm–285 nm is detected by the laser induced fluorescence method. The rovibronic molecular parameters of the X_1 state and B state are derived by analyzing the recorded spectra of the (0, 0) and (1, 0) bands of PbF $B^2\Sigma^+$–$X_1{}^2\Pi_{1/2}$ transition. Also, the lifetimes of B ($v' = 0, 1$) state are discussed from the fluorescence decay spectra. Finally, based on the obtained results in the present work, the Franck–Condon factors of B–X_1 transition of PbF are calculated and compared with that obtained by the Morse potential and RKR/LEVEL methods.

Acknowledgement

Project supported by the National Natural Science Foundation of China (Grant Nos. 11674096 and 11874151).

References

[1] Sasmal S, Talukdar K, Nayak M K, Vaval N and Pal S 2017 *Mol. Phys.* **115** 2807
[2] Chubukov D V, Skripnikovy L V and Labzowsk L N 2019 *JETP Lett.* **110** 382
[3] Skripnikov L V, Kudashov A D, Petrov A N and Titov A V 2014 *Phys. Rev. A* **90** 064501
[4] Rochester G D 1938 *Proc. Roy. Soc. A* **167** 567
[5] Reddy Y P and Rao P T 1967 *Proc. Int. Conf. Spectrosc.* Bombay **1** 129
[6] Singh O Nath, Singh I S and Singh O N 1972 *Can. J. Phys.* **50** 2206
[7] Lumley D J W and Barrow R F 1977 *J. Phys. B: Atom. Molec. Phys.* **10** 1537
[8] Balasubramanian K 1985 *J. Chem. Phys.* **83** 2311
[9] Chen J and Dagdigian P J 1992 *J. Chem. Phys.* **96** 1030
[10] Ziebarth K, Setzer K D, Shestakov O and Fink E H 1998 *J. Mol. Specsc.* **191** 108
[11] McRaven C P, Sivakumar P and Shafer-Ray N E 2007 *Phys. Rev. A* **75** 024502
[12] McRaven C P, Sivakumar P, Shafer-Ray N E, Hall G E and Sears T J 2010 *J. Mol. Specsc.* **262** 89
[13] Baturo V V, Rupasinghe P M, Sears T J, Mawhorter R J, Grabow J U and Petrov A N 2021 *Phys. Rev. A* **104** 012811
[14] Frank A and Rivera A L 2000 *Phys. Rev. A* **61** 054102
[15] Rydberg R 1931 *Z. Phys.* **73** 376
[16] Klein O 1932 *Z. Phys.* **76** 226
[17] Rees A L G 1947 *Prog. Phys. Soc.* **59** 998
[18] Castano F, Juan J de and Martinez E 1983 *J. Chem. Educ.* **60** 91
[19] Le Roy R J 2017 *J. Quantum Spectrosc. Radia. Transfer* **186** 167
[20] Le Roy R J 2000 L *EVEL 7.1 University of Wisconsin Theoretical Chemistry Institute Report CP-642 R*
[21] Barrow R F, Buttler D, Johns J W C and Powell J L 1959 *Proc. Phys. Soc.* **73** 317
[22] Sivakumar P 2009 *Toward measuring a charge-parity violating Electric dipole moment of the electron: production and pseudo-continuous resonance enhanced multiphoton ionization of* $^{208}Pb^{19}F$, Ph.D. Dissertation (Oklahoma: University of Oklahoma)
[23] Western C M 2017 *J. Quantum Spectrosc. Radia. Transfer* **186** 221
[24] Herzberg G 1950 *Molecular Spectra and Molecular Structure. I. Spectra of Diatomic Molecules* (London: D. Van Nostrand Co.) pp. 561–562